Alignment of solid targets under extreme tight focus conditions generated by an ellipsoidal plasma mirror

Deepak Kumar[a], Michal Šmíd[a,1], Sushil Singh[a], Alexander Soloviev[b], Hannes Bohlin[a], Konstantin Burdonov[b], Gashaw Fente[a,2], Alexander Kotov[b], Livia Lancia[c], Vit Lédl[d], Sergey Makarov[e], Michael Morrissey[a], Sergey Perevalov[b], Denis Romanovsky[b], Sergey Pikuz[e], Ryousuke Kodama[f], David Neely[g], Paul McKenna[h], Tomáš Laštovička[a], Mikhail Starodubtsev[b], Stefan Weber[a], Motoaki Nakatsutsumi[i], Julien Fuchs[c]

[a] *ELI Beamlines, Institute of Physics, 5. května 835, 252 41 Dolní Břežany, Czech Republic.*
[b] *Institute of Applied Physics of the Russian Academy of Sciences (IAP RAS), 46 Ulyanov Street, 603950, Nizhny Novgorod, Russia.*
[c] *LULI - CNRS, Ecole Polytechnique, CEA: Universit Paris-Saclay; UPMC Univ Paris 06: Sorbonne Universities, F-91128, Palaiseau cedex, France.*
[d] *Research center Toptec, Institute of Plasma Physics, Sobotecká 1660, 511 01 Turnov.*
[e] *Joint Institute for High Temperatures Russian Academy of Science(JIHT RAS), Moscow, 125412, Russia.*
[f] *Division of Electrical, Electronic and Information Engineering, Graduate School of Engineering, Osaka University, Japan.*
[g] *Central Laser Facility, STFC Rutherford Appleton Laboratory, Didcot OX11 0QX, United Kingdom.*
[h] *Department of Physics SUPA, University of Strathclyde, Glasgow G4 0NG, United Kingdom.*
[i] *European XFEL GmbH, Holzkoppel 4, 22869 Schenefeld, Germany.*

Abstract

The design of ellipsoidal plasma mirrors (EPM) for the PEARL laser facility is presented. The EPM achieved a magnification of 0.32 in the focal spot size and the corresponding increase in focused intensity is expected to be ~ 8. Designing and implementing such focusing optics for short pulse (< 100 fs) systems paves the way for their use in future high power facilities where they can be used to achieve intensities beyond 10^{23} W/cm^2. A retro-imaging based target alignment system is also described, which is used to align solid targets at the output of the ellispoidal mirrors (numerical aperture of 0.75 in this case).

Email address: Deepak.Kumar@eli-beams.eu (Deepak Kumar)
[1] Current affiliation: Helmholtz-Zentrum Dresden-Rossendorf, Bautzner Landstrasse 400, 01328 Dresden, Germany.
[2] Current affiliation: Space Micro Inc., San Diego, California, USA.

Keywords: High intensity laser matter interaction, Ellipsoidal plasma mirror, tight focus, retro alignment.
2018 MSC: 00-00, 00-00

1. Introduction

The consistent technological development of high intensity short pulse lasers and the corresponding improvement in focused intensity over the last few decades have led to the exploration of new frontiers of basic science and applications[1]. Current generation of petawatt (PW) class lasers provide focused intensities around $\sim 10^{21-22}$ W/cm^2 with traditional focusing optics of about f/3. In upcoming facilities like Apollon[2], ELI pillars[3, 4, 5], etc. the corresponding focused intensities will increase to about $\sim 10^{22-23}$ W/cm^2. **However, the ability to achieve higher intensities of the order of 10^{23-24} W/cm^2 will enable the possibility of exploring novel phenomena like radiation reaction[6] and ion acceleration to relativistic energies[7]. Laser plasma interaction in the radiation reaction dominated regime is qualitatively different from the currently achievable regimes of focused intensities $\lesssim 10^{22}$ W/cm^2 because the energy radiated by the oscillating electrons at the focus is comparable to the energy the electrons gain from the laser field. Consequently, a significant fraction of the laser energy is expected to be emitted in multi-MeV X-rays[8, 9].** Thus it will be highly beneficial to increase the achievable intensities, for e.g., by tightly focusing the laser beam to a spot size of the order of the laser wavelength. To achieve this, scientists have either used a small f-number parabola[10] or an ellipsoidal plasma mirror (EPM)[11, 12, 13, 14]. Because of debris damage to the parabola and the associated financial implications, using a small f-number parabola is not a viable option for upcoming facilities like ELI Beamlines[3]. Thus the performance of the EPMs on currently available PW class short pulse lasers is being studied to gain valuable experience in pursuing this technology on future high intensity laser facilities.

An EPM is a small mirror designed to be placed after the focus of the main focusing element. It images the first focus into the second one with a significantly smaller f-number in order to **reduce** the focal spot. The EPM acts in the plasma mirror regime with very high irradiance on the surface and so is a single-use optic. Since 2010, when the first use of the EPM on short pulse lasers was demonstrated[11], there has been steady experience gained on the use of such optics on glass laser systems with pulse lengths of the order of a ps[12, 13]. The optimal geometrical parameters like eccentricity and angle of incidence of the EPM to achieve the desired **magnification** under paraxial approximation have been described earlier[15]. The only remaining parameter for designing the EPM is its scale size, which is set to optimize the reflectivity of the main laser pulse on the EPM[13]. **This paper describes the design of an EPM for the PEARL laser facility[16, 17] at Nizhny Novgorod, Russia. The laser uses large-aperture nonlinear DKDP crystal for optical parametric amplification of the main pulse at a central wavelength of** 910 **nm and provides a maximum energy of** $\lesssim$ 20 **J. A four grating compressor with a total efficiency of about** 77% **compresses the beam to a pulse duration of** $\sim$ 60 **fs. The main beam, which has a diameter of about** 18 **cm, is then focused using an f/**2 **parabola**. The EPM was coupled to the focus of **the off-axis parabola (OAP)** to tightly focus the beam with a numerical aperture of 0.75 at the output. To the best of our knowledge, this is the first instance of using the EPM on a short pulse ($<$ 100 fs) laser system.

For such a tightly focused spot, the front surface of the solid target needs to be positioned within the Rayleigh length of about 2 μm (for a diffraction limited spot). This is a challenging requirement because many precision measurement devices are not suitable for the harsh laser-plasma environment. For e.g., several encoders like the resistive or magnetic encoders are susceptible to electro-magnetic pulse (EMP). Thus optical methods for aligning the target are often used. In many such cases the rear surface of the target is aligned with respect to a reference (for e.g., a microscope objective or a chromatic confocal sensor). Then the target is translated by a distance equal to its thickness in

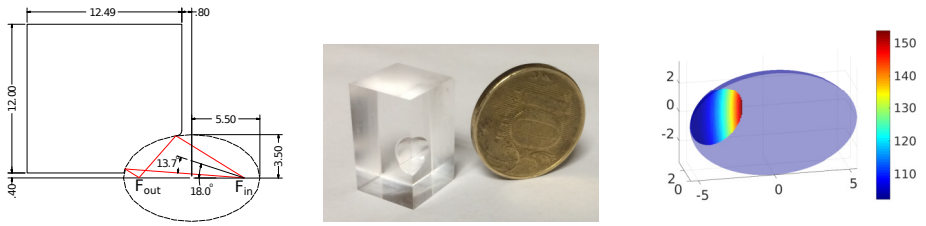

(a) (b) (c)

Figure 1: (a) Sectional view of the EPM depicting the geometry. The boundary of the laser beam path is shown in red. F_{in} (F_{out}) is the input (output) focus of the EPM. (b) Image of a machined EPM placed next to a 10 ₽ coin of diameter 17.5 mm. (c) Expected fluence in J/cm^2 on the surface of the EPM when used with the PEARL laser delivering 20 J on target. All dimensions are in mm.

order to align the front surface. An alternative method is to align the front surface of the target with using a retro imaging system which has been demonstrated to work well with precision comparable to the Rayleigh length of the focusing optic[18]. Alignment based on retro reflection has the advantage of being immune to surface irregularities on the target introduced while mounting the target. This paper describes a retro imaging system for aligning a solid target to the tightly focused output from an EPM. The performance of the retro alignment system is bench-marked against an alternative alignment technique based on monitoring the near field of the beam being obstructed by the target.

This paper is structured as follows. Section 2 describes the geometry of the EPMs and characterizes their performance. Section 3 describes two different procedures for aligning the target at the output focus of the EPM. Finally, the paper concludes with section 4.

2. EPM geometry and performance characterization

Geometry of the EPM. The EPMs designed for the PEARL campaign had a major axis of 5.5 mm and a minor axis of 3.5 mm as shown in figure 1a. The axis of the EPM was oriented at an incident angle of 18° with respect to the axis of the incoming beam focused by an f/2 parabola. Such a geometry transforms

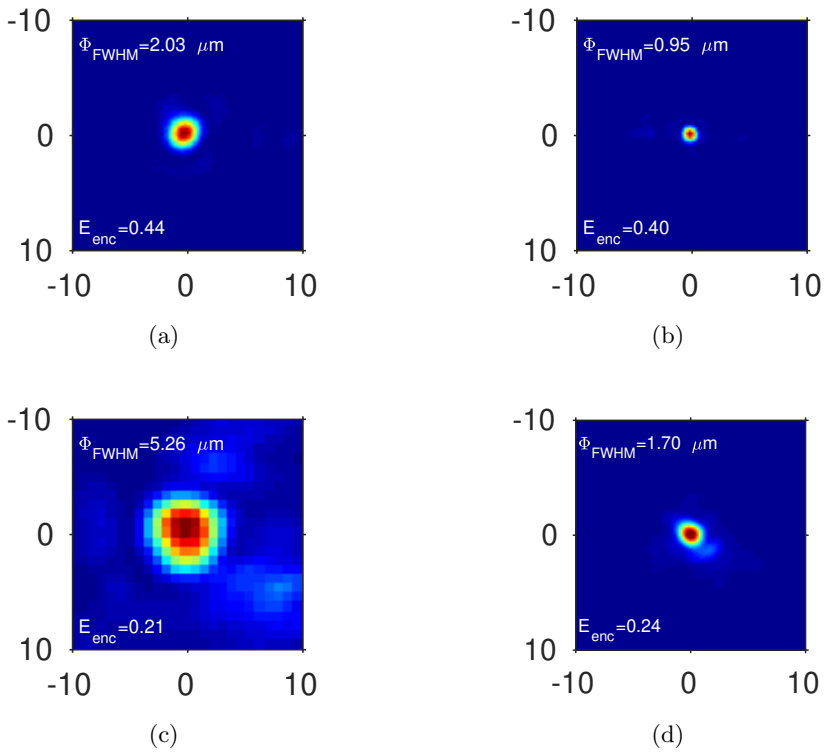

Figure 2: Focal spot images characterizing the performance of the EPMs. Focal spot at the input (a) and at the output (b) of the EPM at the test bench. Focal spot at the input (c) and at the output (d) of the EPM at the PEARL laser facility as measured with low power alignment beam. Field of view in all the images is 20 μm$\times$20 μm. The diameter of the full width at half maximum (FWHM) of the focal spot (Φ_{FWHM}) and the fraction of energy enclosed within the FWHM (E_{enc}) is mentioned in each image.

the input beam numerical aperture of 0.24 to an output numerical aperture of 0.75, i.e., an expected magnification of approximately 0.3[15]. The EPM was machined by single point diamond turning from a polymethyl methacrylate (PMMA) substrate. An example of a machined EPM is shown in figure 1b. For the geometry of the EPM described above, the expected fluence on the surface of the EPM was calculated when used with the PEARL laser (20 J, 60 fs) and is shown in figure 1c. For an average fluence of about 110 J/cm^2, we expect a reflectivity of about $60-70\%$[19].

Characterization of the EPM. The EPMs were characterized in a non-plasma regime on a test bench where a collimated 5 cm diameter HeNe laser beam was focused by an f/2 OAP. The setup was similar to that described by Wilson et al[13] and the f-number of the parabola matched that of the PEARL facility. The **focal spots produced** by the EPM on the test bench and also on the PEARL laser facility are shown in figure 2. On the test bench the measured **magnification** was about 0.48, significantly weaker than the predicted **magnification** of 0.3. **In order to explain this discrepancy, we are currently developing optical models which calculate exact solution of focused intensity in the non-paraxial regime and also incorporate wavefront errors[20].** On the PEARL facility the observed **magnification** was 0.32. The corresponding increase in focused intensity that can be expected **at the PEARL laser facility** is about 8 when compared to operation of the laser with normal f/2 OAP[13, 11]. When compared to a setup including a planar plasma mirror operating at similar fluence, the expected enhancement of intensity is even higher ≈ 11.

3. Target alignment: setup and results

Setup for alignment. The EPM and the target at the second focus were mounted on 3-axis motorized linear stages with picomotor actuators (Model number 8302 from Newport Corporation). The picomotors had a minimum step size of < 30 nm and thus were very useful in precisely aligning the EPM and the target. The setup of the EPM and targetry stages is shown in figure 3. In order to align the front surface of the target, a retro imaging system was assembled as shown in the figure. The laser light reflected from the front surface of the target is collected by the EPM. The pellicle beam splitter of thickness 5 μm then reflects the light which is then focused by a retro imaging lens on to a camera. The retro imaging lens used in the setup had a focal length of 10 cm and an aperture of 7.5 cm. Such high f-number lens enabled collecting all the light reflected from the pellicle and also ensured a desired magnification of about 10 by the lens

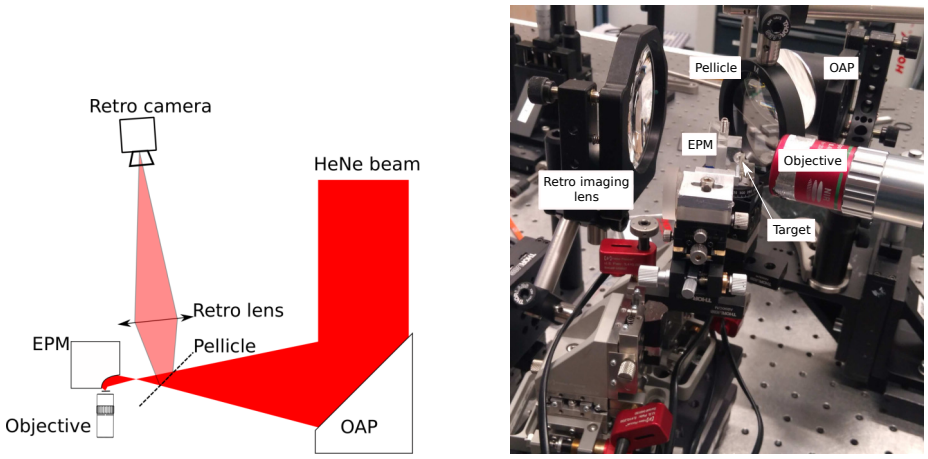

(a) (b)

Figure 3: (a) Schematic of the setup used on the test bench to characterize the EPMs and bench mark the retro alignment system. (b) Image of the setup showing the physical layout of the components.

within a reasonable space.

A similar setup for mounting the EPM and the target was also used for real laser-plasma experiments at the PEARL laser facility. The retro imaging system was not installed at the PEARL facility as only thin targets were shot as discussed in the next paragraph.

Target alignment by monitoring the near field. At the PEARL laser facility, 3 μm thick Al foils were aligned to the output focus of the EPM. The target thickness was comparable to the Rayleigh length and so, the target was aligned by monitoring the near field after the EPM focus as shown in figure 4a. The microscope objective used for aligning the EPM was defocused and used as a lens for monitoring the near field. The near field images obtained during the alignment procedure are shown in figure 4b. As the target moves to intercept the incoming alignment beam, the shadow of the target is clearly visible in the near field. The direction from where the shadow enters the near field image depends on whether the target is in front or behind the focus. When a thin

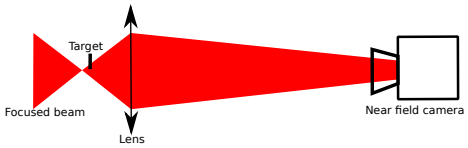

(a)

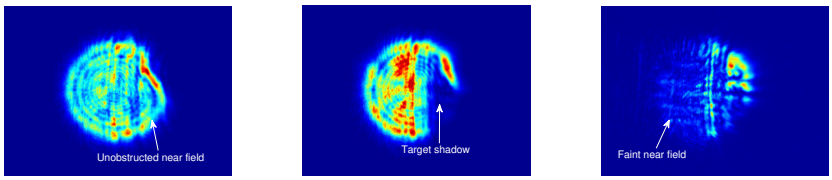

(b)

Figure 4: Target alignment by monitoring the near field. (a) Schematic of the alignment method. (b) Near field images during target alignment at PEARL facility showing unobstructed near field, shadow of target moving from the right and shadow of the near field when target is at focus.

target is at the focus, the entire near field profile diminishes simultaneously as seen in the figure (4b, right). If the target thickness (3 μm in our case) is comparable to the Rayleigh length (expected to be around 3 μm for the output of EPM at the PEARL facility) then two shadows approaching from either side on the near field can also be observed and the shadow from the front side of the target (figure 4b center) can be distinguished from the shadow from the rear side of the target. On the PEARL facility, front side of the targets were aligned by monitoring the shadow from the front surface and placing the front surface at the focus. When shot with the full energy beam, a significant increase in the X-rays and the maximum ion energy were measured as compared to normal OAP shots. These results will be described in subsequent publications.

Target alignment by retro imaging. The retro imaging system, which is useful for aligning thicker targets was assembled only on the test bench in order to bench-mark its performance. A 0.8 μm thick Al target was chosen to compare

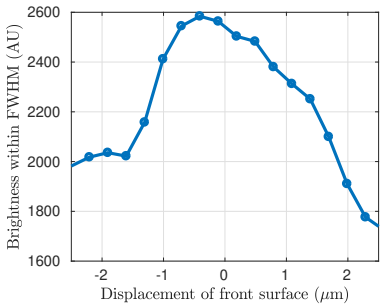

Figure 5: Average brightness of the spot measured on the retro imaging camera as a function of the target displacement. A displacement of 0 corresponds to the reference location of the target where it was aligned by monitoring the near field.

the two alignment procedures, as the target thickness was comparable to the Rayleigh length on the test bench (see figure 2b). Initially the target was aligned at the focus by monitoring the near field as described in the previous paragraph. Subsequently, the axial location of the target was varied around this reference location. The location of the target was absolutely measured using a Fabry-Pérot interferometer based displacement sensor. Figure 5 shows the average brightness of the measured spot on the retro imaging camera as a function of target displacement. The result shows that optimizing the target location for maximizing the average intensity measured in the retro imaging camera can be used for aligning the target at the focus of the EPM within the Rayleigh length (approximately ± 1 μm on the test bench). Such a retro imaging system is planned to be implemented on future campaigns involving thicker targets with EPMs. **It should be noted that on high power facilities, the pellicle will have to be removed from the beam path before the full power shot in order to avoid the beam wavefront distortion due to nonlinear interaction of high intensity laser beam with the pellicle.**

Retro imaging setups on existing facilities[18] utilize the focusing OAP to collect light reflected from the target front surface. However, the retro imaging setup described in this paper uses the EPM to collect the reflected light. The EPM in this configuration for collecting the reflected light acts like a high mag-

nification objective to create an image at the front focus which is then imaged on the retro imaging camera with a lens. The pellicle beamsplitter used in the alignment process introduces significant wavefront errors in the reflected light, but as is evident from figure 5 the alignment procedure is still robust.

4. Conclusion

This paper presents the design of EPM for PEARL laser facility and the retro-focus alignment procedure for aligning solid targets to the focus of the EPM. Measurement of the focal spots before and after the EPM on the PEARL facility yield an expected enhancement in intensity of ~ 8 during its operation. For a tightly focused beam at the output of the EPM, the Rayleigh length is extremely small (≈ 2 μm) and front surface of solid targets have to be aligned within this precision. Two different methods for aligning the target at the focus of the EPM were described. The retro imaging system which aligns the target by collecting the reflected light was shown to have a precision of alignment within the Rayleigh length.

Acknowledgments

The results of the Project LQ1606 were obtained with the financial support of the Ministry of Education, Youth and Sports as part of targeted support from the National Programme of Sustainability II. This research was also sponsored by the Czech Science Foundation (project No. 18-09560S), by the project High Field Initiative (CZ.02.1.01/0.0/0.0/15_003/0000449) from European Regional Development Fund (HIFI) and by the Ministry of Education and Science of the Russian Federation under Contract No.14.Z50.31.0007. **The work was also supported by the Ministry of Education and Science of the Russian Federation (FTP grant #14.607.21.0196, project ID: RFMEFI60717X0196). The work of JIHT RAS team was done in the frame of the state assignment of FASO of Russia to JIHT RAS (topic #01201357846).**

References

[1] G. A. Mourou, T. Tajima, S. V. Bulanov, Optics in the relativistic regime, Rev. Mod. Phys. 78 (2006) 309–371. doi:10.1103/RevModPhys.78.309.
URL https://link.aps.org/doi/10.1103/RevModPhys.78.309

[2] D. Papadopoulos, J. Zou, C. Le Blanc, G. Chériaux, P. Georges, F. Druon, G. Mennerat, P. Ramirez, L. Martin, A. Fréneaux, et al., The Apollon 10 PW laser: experimental and theoretical investigation of the temporal characteristics, High Power Laser Science and Engineering 4 (2016) e34. doi:10.1017/hpl.2016.34.

[3] S. Weber, S. Bechet, S. Borneis, L. Brabec, M. Bučka, E. Chacon-Golcher, M. Ciappina, M. DeMarco, A. Fajstavr, K. Falk, E.-R. Garcia, J. Grosz, Y.-J. Gu, J.-C. Hernandez, M. Holec, P. Janečka, M. Jantač, M. Jirka, H. Kadlecova, D. Khikhlukha, O. Klimo, G. Korn, D. Kramer, D. Kumar, T. Laštovička, P. Lutoslawski, L. Morejon, V. Olšovcová, M. Rajdl, O. Renner, B. Rus, S. Singh, M. Šmid, M. Sokol, R. Versaci, R. Vrána, M. Vranic, J. Vyskočil, A. Wolf, Q. Yu, P3: An installation for high-energy density plasma physics and ultra-high intensity lasermatter interactio Matter and Radiation at Extremes 2 (4) (2017) 149 – 176. doi:10.1016/j.mre.2017.03.003.
URL http://www.sciencedirect.com/science/article/pii/S2468080X17300171

[4] S. Gales, D. L. Balabanski, F. Negoita, O. Tesileanu, C. A. Ur, D. Ursescu, N. V. Zamfir, New frontiers in nuclear physics with high-power lasers and brilliant monochromatic gamma beams, Physica Scripta 91 (9) (2016) 093004.
URL http://stacks.iop.org/1402-4896/91/i=9/a=093004

[5] S. Kühn, M. Dumergue, S. Kahaly, S. Mondal, M. Füle, T. Csizmadia, B. Farkas, B. Major, Z. Várallyay, E. Cormier, M. Kalashnikov, F. Calegari, M. Devetta, F. Frassetto, E. Månsson, L. Poletto, S. Stagira, C. Vozzi, M. Nisoli, P. Rudawski, S. Maclot, F. Campi,

H. Wikmark, C. L. Arnold, C. M. Heyl, P. Johnsson, A. LHuillier, R. Lopez-Martens, S. Haessler, M. Bocoum, F. Boehle, A. Vernier, G. Iaquaniello, E. Skantzakis, N. Papadakis, C. Kalpouzos, P. Tzallas, F. Lpine, D. Charalambidis, K. Varjú, K. Osvay, G. Sansone, The ELI-ALPS facility: the next generation of attosecond sources, Journal of Physics B: Atomic, Molecular and Optical Physics 50 (13) (2017) 132002.
URL http://stacks.iop.org/0953-4075/50/i=13/a=132002

[6] S. V. Bulanov, T. Z. Esirkepov, D. Habs, F. Pegoraro, T. Tajima, Relativistic laser-matter interaction and relativistic laboratory astrophysics, The European Physical Journal D 55 (2) (2009) 483. doi:10.1140/epjd/e2009-00138-1.
URL https://doi.org/10.1140/epjd/e2009-00138-1

[7] T. Esirkepov, M. Borghesi, S. V. Bulanov, G. Mourou, T. Tajima, Highly efficient relativistic-ion generation in the laser-piston regime, Phys. Rev. Lett. 92 (2004) 175003. doi:10.1103/PhysRevLett.92.175003.
URL https://link.aps.org/doi/10.1103/PhysRevLett.92.175003

[8] T. Nakamura, J. K. Koga, T. Z. Esirkepov, M. Kando, G. Korn, S. V. Bulanov, High-power γ-ray flash generation in ultraintense laser-plasma interactions, Phys. Rev. Lett. 108 (2012) 195001. doi:10.1103/PhysRevLett.108.195001.
URL http://link.aps.org/doi/10.1103/PhysRevLett.108.195001

[9] C. P. Ridgers, C. S. Brady, R. Duclous, J. G. Kirk, K. Bennett, T. D. Arber, A. P. L. Robinson, A. R. Bell, Dense electron-positron plasmas and ultraintense γ rays from laser-irradiated solids, Phys. Rev. Lett. 108 (2012) 165006. doi:10.1103/PhysRevLett.108.165006.
URL http://link.aps.org/doi/10.1103/PhysRevLett.108.165006

[10] S.-W. Bahk, P. Rousseau, T. A. Planchon, V. Chvykov, G. Kalintchenko, A. Maksimchuk, G. A. Mourou, V. Yanovsky,

Generation and characterization of the highest laser intensities (10^{22} w/cm^2), Opt. Lett. 29 (24) (2004) 2837–2839. doi:10.1364/OL.29.002837.
URL http://ol.osa.org/abstract.cfm?URI=ol-29-24-2837

[11] M. Nakatsutsumi, A. Kon, S. Buffechoux, P. Audebert, J. Fuchs, R. Kodama, Fast focusing of short-pulse lasers by innovative plasma optics toward extreme intensity, Opt. Lett. 35 (13) (2010) 2314–2316. doi:10.1364/OL.35.002314.
URL http://ol.osa.org/abstract.cfm?URI=ol-35-13-2314

[12] M. Nakatsutsumi, Y. Sentoku, A. Korzhimanov, S. N. Chen, S. Buffechoux, A. Kon, B. Atherton, P. Audebert, M. Geissel, L. Hurd, M. Kimmel, P. Rambo, M. Schollmeier, J. Schwarz, M. Starodubtsev, L. Gremillet, R. Kodama, J. Fuchs, Self-generated surface magnetic fields inhibit laser-driven sheath acceleration of high-energy protons, Nature Communications 9 (280). doi:10.1038/s41467-017-02436-w.
URL https://doi.org/10.1038/s41467-017-02436-w

[13] R. Wilson, M. King, R. J. Gray, D. C. Carroll, R. J. Dance, C. Armstrong, S. J. Hawkes, R. J. Clarke, D. J. Robertson, D. Neely, P. McKenna, Ellipsoidal plasma mirror focusing of high power laser pulses to ultra-high intensities, Physics of Plasmas 23 (3). doi:http://dx.doi.org/10.1063/1.4943200.
URL http://scitation.aip.org/content/aip/journal/pop/23/3/10.1063/1.4943200

[14] R. Wilson, M. King, R. J. Gray, D. C. Carroll, R. J. Dance, N. M. H. Butler, C. Armstrong, S. J. Hawkes, R. J. Clarke, D. J. Robertson, C. Bourgenot, D. Neely, P. McKenna, Development of focusing plasma mirrors for ultraintense laser-driven particle and radiation sources, Quantum Beam Science 2 (1). doi:10.3390/qubs2010001.
URL http://www.mdpi.com/2412-382X/2/1/1

[15] A. Kon, M. Nakatsutsumi, S. Buffechoux, Z. L. Chen, J. Fuchs, Z. Jin, R. Kodama, Geometrical optimization of an ellipsoidal plasma mirror toward tight focusing of ultra-intense laser puls

Journal of Physics: Conference Series 244 (3) (2010) 032008.
URL http://stacks.iop.org/1742-6596/244/i=3/a=032008

[16] V. V. Lozhkarev, G. I. Freidman, V. N. Ginzburg, E. V. Katin, E. A. Khazanov, A. V. Kirsanov, G. A. Luchinin, A. N. Mal'shakov, M. A. Martyanov, O. V. Palashov, A. K. Poteomkin, A. M. Sergeev, A. A. Shaykin, I. V. Yakovlev, Compact 0.56 petawatt laser system based on optical parametric chirped pulse amplification in KD*P cr Laser Physics Letters 4 (6) 421–427. arXiv:https://onlinelibrary.wiley.com/doi/pdf/10.1002/lapl.200710008, doi:10.1002/lapl.200710008.
URL https://onlinelibrary.wiley.com/doi/abs/10.1002/lapl.200710008

[17] A. and Soloviev, K. Burdonov, S. N. Chen, A. Eremeev, A. Korzhimanov, G. V. Pokrovskiy, T. A. Pikuz, G. Revet, A. Sladkov, V. Ginzburg, E. Khazanov, A. Kuzmin, R. Osmanov, I. Shaikin, A. Shaykin, I. Yakovlev, S. Pikuz, M. Starodubtsev, J. Fuchs, Experimental evidence for short-pulse laser heating of solid-density target to high bulk temperatures, Scientific Reports 7 (2017) 12144. doi:10.1038/s41598-017-11675-2.
URL https://doi.org/10.1038/s41598-017-11675-2

[18] D. C. Carroll, M. Coury, G. Scott, P. McKenna, M. Streeter, H. Nakamura, Z. Najmudin, F. Fiorini, S. Green, J. Green, P. Foster, R. Heathcote, K. Poder, D. Symes, R. J. Clarke, R. Pattathil, D. Neely, An assessment of the reproducibility of the gemini retro focusing system, Tech. rep., Central Laser Facility Annual Report (2011).
URL https://www.clf.stfc.ac.uk/Pages/ar10-11_lsd_astra.pdf

[19] G. Doumy, F. Quéré, O. Gobert, M. Perdrix, P. Martin, P. Audebert, J. C. Gauthier, J.-P. Geindre, T. Wittmann, Complete characterization of a plasma mirror for the production of high-contrast ultraintense laser pulse Phys. Rev. E 69 (2004) 026402. doi:10.1103/PhysRevE.69.026402.
URL http://link.aps.org/doi/10.1103/PhysRevE.69.026402

[20] T. M. Jeong, S. Weber, B. L. Garrec, D. Margarone, T. Mocek, G. Korn, Spatio-temporal modification of femtosecond focal spot under tight focusing condition, Opt. Express 23 (9) (2015) 11641–11656. doi:10.1364/OE.23.011641.
URL http://www.opticsexpress.org/abstract.cfm?URI=oe-23-9-11641